

Martin-Puplett Interferometric Measurements of Bunch Length at the A0 Photo-Injector

Author: John Daniel Hlotke

Supervisor: Randy Thurman-Keup

Bunch length measurements of the A0 photo-injector have recently been taken utilizing streak cameras. Limited to detecting bunch lengths greater than about one picosecond, a Martin-Puplett interferometer was installed to begin taking measurements for smaller anticipated bunch lengths. The correlation between the streak camera and the interferometer for large (2-14 picosecond) bunch lengths was studied this summer as well as the applicability of using an interferometer for bunch length measurement greater than one picosecond.

The interferometer setup is depicted in Fig. 1 and Fig. 2.

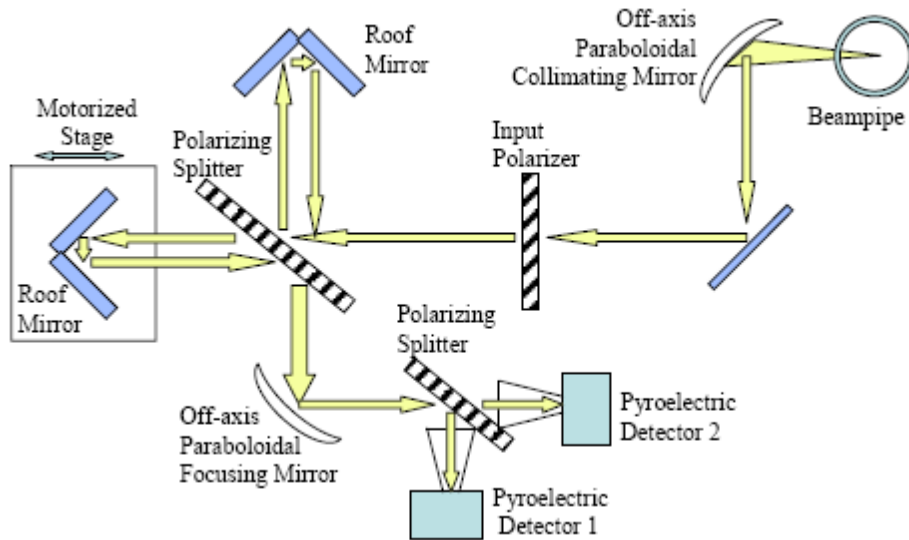


Figure 1: Schematic of the Interferometer Setup

Thurman-Keup, Filler, Kazakevich. Fermilab. Bunch Length Measurement at the A0 Photo-Injector using a Martin-Puplett Interferometer. <http://ss.fnal.gov/archive/2008/pub/fermilab-pub-08-115-ad.pdf>

Electromagnetic radiation is generated by passing electron bunches through optical transition radiation (OTR) screens. As the electrons pass through these screens, the change in the dielectric constant of the surrounding material causes electromagnetic radiation to be emitted. This radiation is then fed to the interferometer along an optical path. Incoming radiation is polarized by the first wire grid. Any electric field component perpendicular to the grid is passed, while any parallel component induces an opposing current in the wires that causes a reflection of the parallel component. The second polarizing grid operates in the same fashion and splits the light down two different paths. The roof mirrors swap the polarization of the plane waves so that the radiation

that was originally transmitted by the grid is reflected when it returns, and vice versa. Both path lengths end with roof mirrors, one fixed the other moveable.

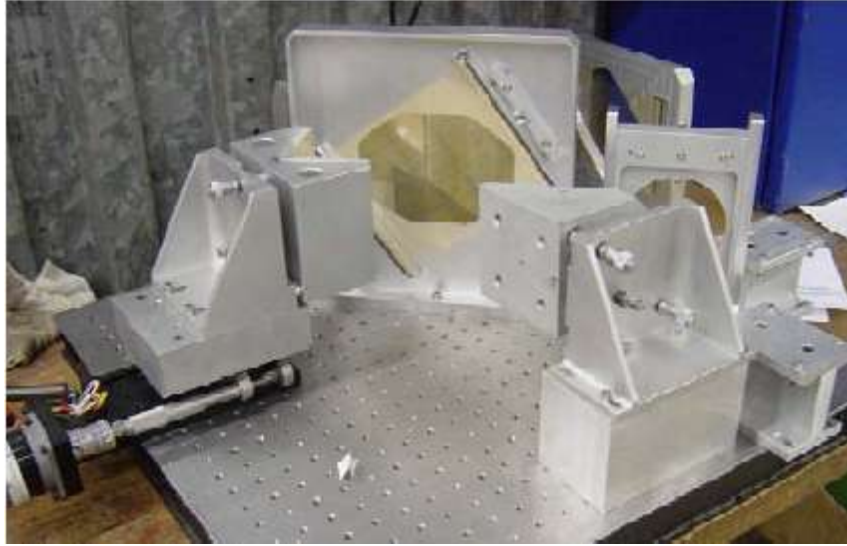


Figure 2: Photograph of the Martin-Puplett Interferometer

Thurman-Keup, Filler, Kazakevich. Fermilab. Bunch Length Measurement at the A0 Photo-Injector using a Martin-Puplett Interferometer. <http://lss.fnal.gov/archive/2008/pub/fermilab-pub-08-115-ad.pdf>

By varying the path length of the second leg, the recombined light polarization shifts from circular to elliptical. The electromagnetic radiation is then collected in a parabolic mirror and focused onto a final polarizing wire grid that splits the signal between two pyroelectric detectors that absorb the radiation as heat. The resulting change in temperature produces a current in the crystal detector element that is converted into a measurable voltage. By taking the difference of the two signals and dividing by the sum, an interferogram is produced that is less sensitive to beam intensity changes than a similar setup with a single detector.

To develop a better understanding of the effect various parameters had on the reconstructed bunch length, simulations were run using GNU Octave (an open source MATLAB clone). An overview of the relations used in the simulations follows. The interested reader is directed to [1] for a more thorough discussion and derivation. Difference interferograms can be computed from simply knowing the starting charge distribution $\rho(z)$. We first compute the form factor, which is related to the charge distribution by a Fourier transform:

$$F(\omega) = \frac{1}{Q} \int dz \rho(z) e^{-i\omega z}$$

Next, the spectrum of the bunch is calculated using the relation:

$$I(\omega) = I_1(\omega)(N + N(N - 1)|F(\omega)|^2)$$

where N is the number of particles in the bunch and $I_1(\omega)$ is the single particle spectrum intensity. Finally, the difference interferogram is computed:

$$\delta(\tau) = \frac{\int_0^\infty I(\omega) \cos(\omega\tau) d\omega}{\int_0^\infty I(\omega) d\omega}$$

Several simplifications were made for the analysis. We assumed the charge (Q), number of particles (N), and total intensity of the signal ($\int_0^\infty I(\omega) d\omega$) remained constant over the measurement process. In addition, the single particle spectrum is fairly uniform over our measured frequencies and thus can be assumed to be constant. Due to the properties of the Fourier transform, $I(\omega)$ was approximated by $|F(\omega)|^2$. All of these assumptions and approximations have no effect on the final shape of the interferogram, they simply change the amplitude of the final signal produced. Seeing that the numerator of $\delta(\tau)$ is simply the real part of a Fourier transform we have our final equation relating $\rho(z)$ to $\delta(\tau)$:

$$\delta(\tau) = \Re\{\mathcal{F}\{|\mathcal{F}\{\rho(z)\}|^2\}\}$$

The Kramers-Kronig analysis used to reconstruct the bunch shape works well for Gaussian shapes. How well the process worked for non-Gaussian bunches was unknown and a model was desired. In addition, the pyroelectric detectors used in the experiment do not have perfect response curves; they lose sensitivity at low frequencies. In order to model this behavior, we introduced a simple arctangent response curve to model the detector cutoff and varied the frequency at which this response curve dropped to zero. Several different charge distributions were modeled, and the interferograms were passed in to MATLAB code used previously at Fermilab to reconstruct the bunch shape. Figures 3 and 4 show sample bunch shapes, reconstructed bunch shapes, associated spectra, and the interferogram produced. Table 1 shows the reconstructed full width half-max (FWHM) values measured as compared to the original signals FWHM. For most charge distributions, the FWHM from the reconstruction process deviates only 2-3% from the original signal FWHM. The reconstruction process is not so accurate when dealing with Lorentzian or exponential charge distributions. This is due to the fact that a Gaussian fit is used to approximate missing data in the spectrum arising from non-ideal detector response and as such does a bad job of approximating Lorentzian and exponential spectral distributions.

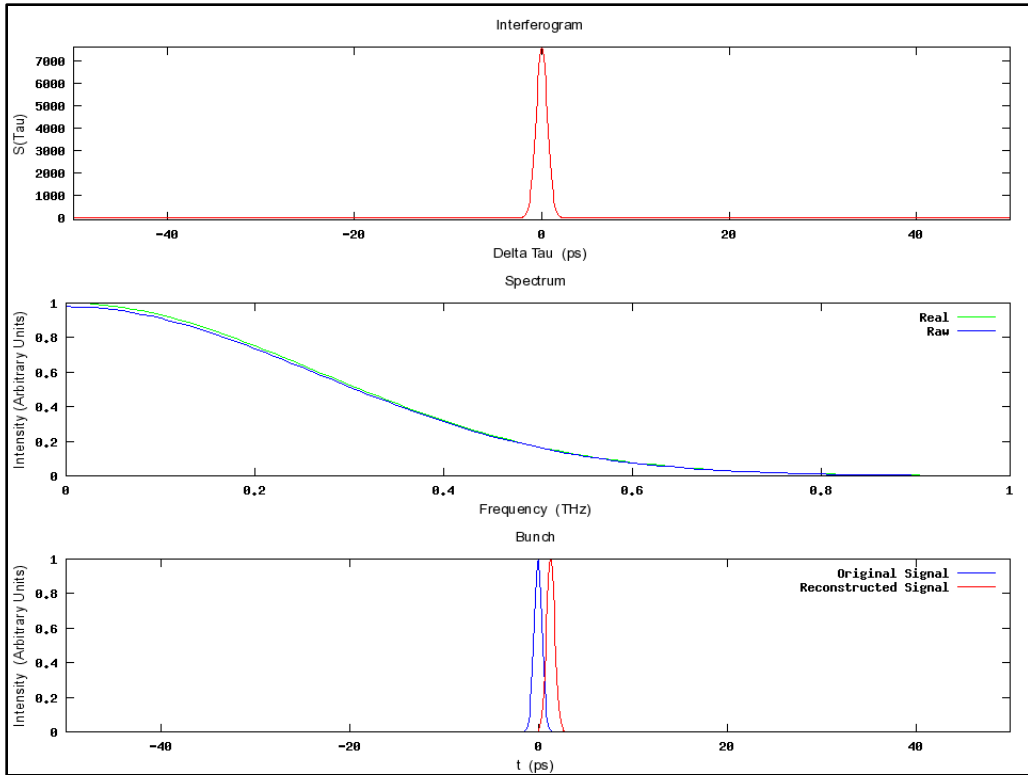


Figure 3: Simulated Gaussian Bunch with Ideal Detector Response

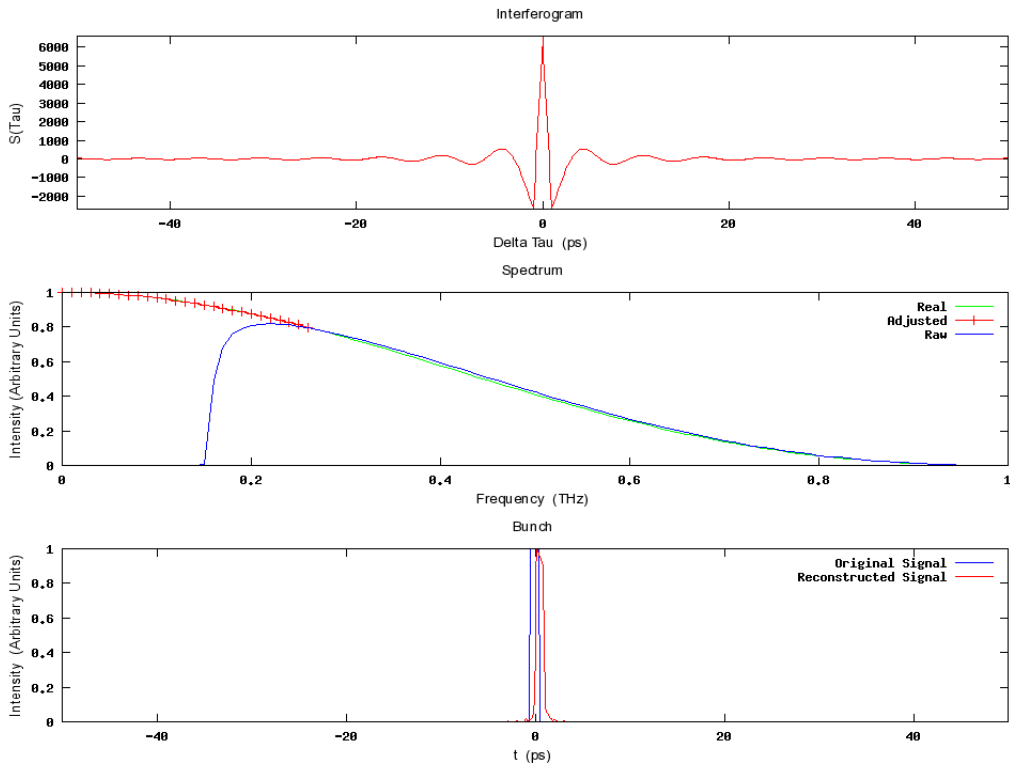


Figure 4: Simulated Square Bunch with 150 GHz Detector Cutoff

Table 1: Simulated Bunch Length Measurements

Shapes	Original FWHM (ps)	Reconstructed FWHM (ps)				
		No cutoff	0 GHz cutoff	50 GHz cutoff	100 GHz cutoff	150 GHz cutoff
Gaussian	1.0008	1.0266	1.0256	1.0267	1.0239	1.0249
Square	1.0000	0.9972	0.9922	0.9877	0.9853	0.9840
Symmetric Triangle	1.0000	1.0754	1.0678	1.0693	1.0714	1.0737
Falling Right Triangle	1.0000	1.0068	0.9848	0.9812	0.9789	0.9788
Falling Exponential	1.0002	1.0656	0.9543	0.8690	0.7855	0.7136
Lorentz	1.0000	1.2650	1.1859	1.1445	1.1038	1.0626
Symmetric Double Gaussian	1.0005	1.0308	1.0322	1.0279	1.0270	1.0285
Asymmetric Double Gaussian	1.0007	1.0320	1.0310	1.0253	1.0241	1.0241

Part of my time spent here at Fermilab was writing the small section of code that deals with cutoff of the detector response. Comparing Figures 3 and 4, one observes that some of the spectral content is lost when a non-ideal detector is used. In order for the Kramers-Kronig analysis to be accurate, the missing spectral information must be interpolated from the remaining data. Prior to my arrival, a simple quadratic fit was being performed to approximate the Gaussian nature of the curve. Since the spectral curve is expected to be Gaussian in nature, a Gaussian extrapolation of the data was desired. The Gaussian probability density function for our data is given by:

$$I = \frac{1}{\sigma\sqrt{2\pi}} e^{-\frac{(\omega-\mu)^2}{2\sigma^2}}$$

The term $\frac{1}{\sigma\sqrt{2\pi}}$ simply ensures that the total area under the curve equals one. Since we are not concerned with this property of a Gaussian distribution, we drop this term. The maximum of our curve is located at μ . For our purposes, this is zero. In order to fit a curve to the data we take the natural logarithm of both sides:

$$\ln I = \frac{-\omega^2}{2\sigma^2}$$

Making a substitution of variables, we can produce a linear equation. Transforming our data set with $y = \ln I$ and $x = \omega^2$ the above becomes:

$$y = -\frac{x}{2\sigma^2}$$

which is easily used with existing MATLAB functions to perform a linear least squares fit to find the parameter $\frac{1}{2\sigma^2}$. Although developing the code for the extrapolation was fairly simple, determining where to begin extrapolating from, and for how many points was not.

In simulations, extrapolation was from a point where the detector response was above 98%. Our detectors have no published response curves that we are aware of, and so the determination of where to extrapolate from for real data is slightly more difficult. The first set of interferograms exhibit a cutoff in detector sensitivity around 125 GHz (See Figure 5). Confusingly, the detector seemed to begin picking up some frequencies again around 75 GHz. Because we do not know the true response curve of the pyroelectric detectors, there is no obvious way to properly incorporate the spike into the Gaussian fit. For our purposes, we choose a point on the larger curve where the signal was still increasing, around 140 GHz. Later interferograms (Figure 6), we saw good detector response in the 75-125 GHz region much to our surprise. The apparent cutoff of the detector at these frequencies had vanished. The only conclusion is that the phenomena could not be due to the pyroelectric detectors alone. Due to the only visible wavelengths being much longer, the extrapolation point needed to be shifted to around 100 GHz illustrating the difficulty in attempting to be consistent with the fitting process.

In order to test the accuracy of the interferometer at longer bunch lengths it was compared to streak camera data taken at the same time. There was no correlation between the two measurements. The interferometer readings would find bunch lengths changing by as much as 1 ps between runs, whereas the streak camera was consistently reading the same value. In addition, the values for the bunch lengths did not agree between devices. It was hypothesized that the quadrupole magnets may have been causing problems with our measurements. Figure 6 was one of several runs where the quadrupole strengths were varied to see what effect the quad's had on the bunch length measurement. When only one quad was varied in strength from 0 to 6 amps, there was no effect on the measured longitudinal bunch length as expected. When the beam was flattened vertically with one quad, the reconstructed bunch length was calculated to be 8 ps. The beam was then flattened horizontally and a second measurement was taken. The reconstructed bunch length was calculated to be 4 ps. The variation of the quad's should not have affected the longitudinal charge distribution, yet we saw a change in the bunch length. This seems to indicate that the interferometer is not accurate for long bunch lengths. Further tests involving variation of the shape of the beam need to be performed.

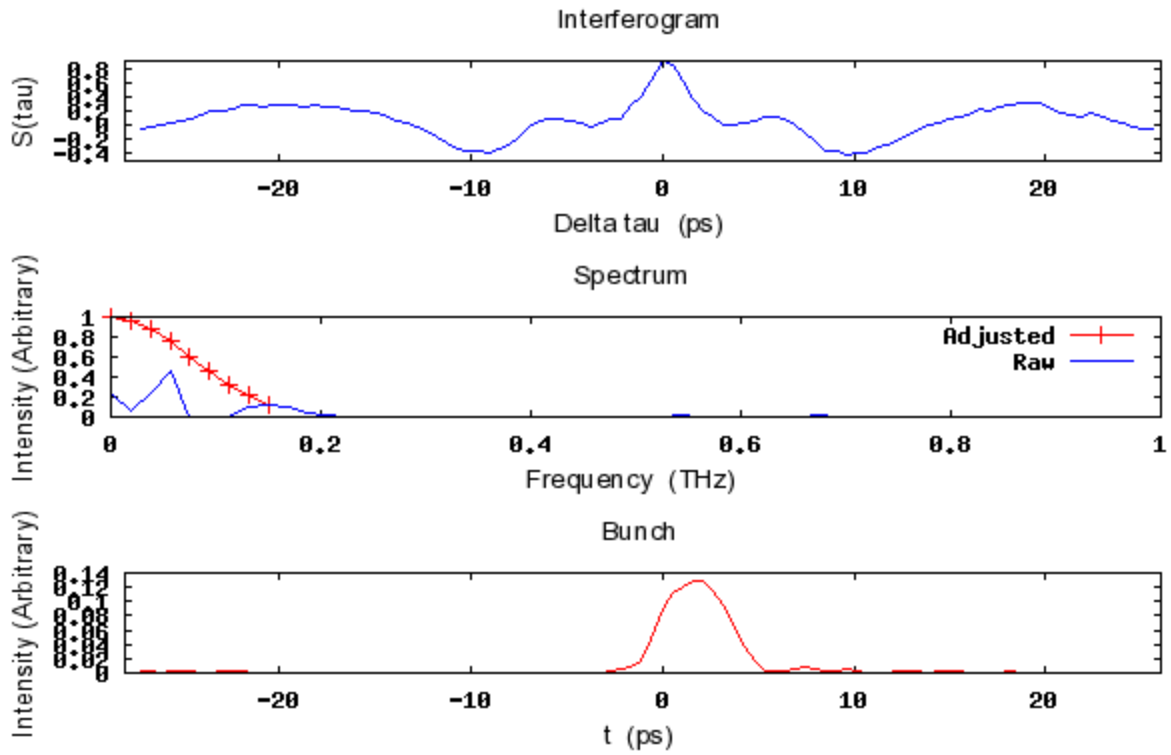


Figure 5: Actual Interferogram Measurement

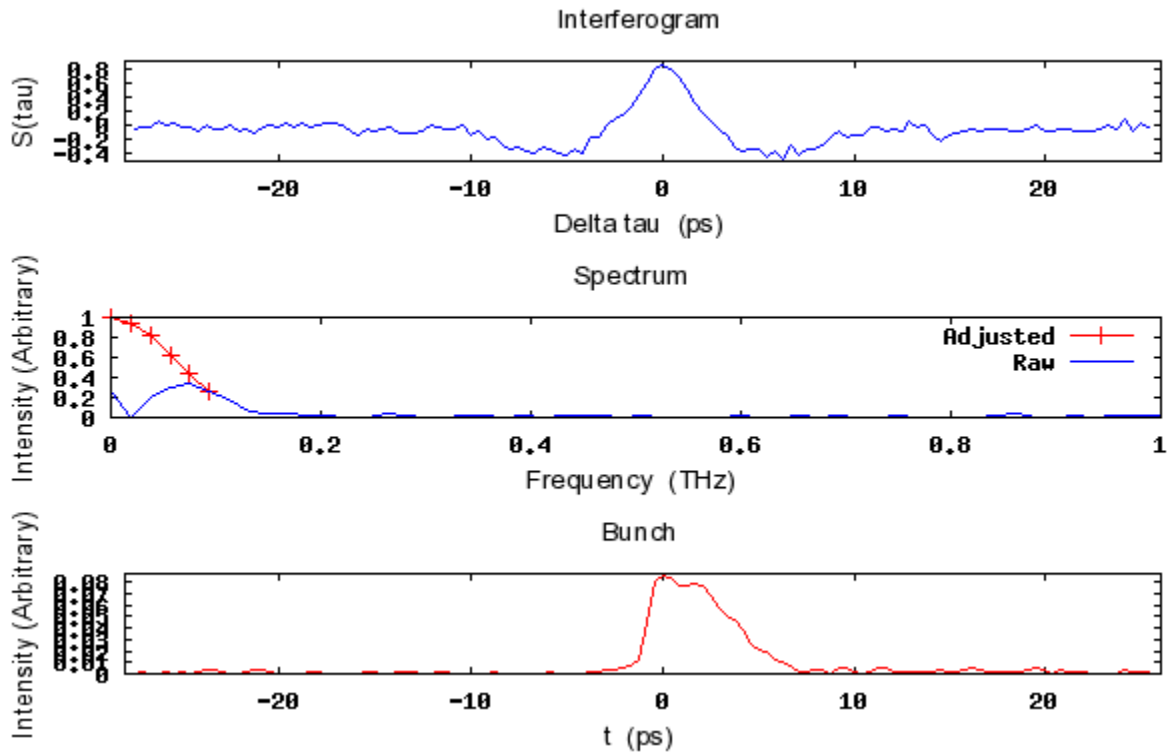


Figure 6: A Second Interferogram Measurement

Two possible issues for the detector response issue were investigated. The first dealt with the fact that the electromagnetic radiation travels outside the beam line in open air. The data was taken during extremely humid days and there was some concern that water vapor was absorbing certain wavelengths. Other interferometer setups have purged the detector and transport lines with dry nitrogen to minimize this effect [1]. Analysis of the absorption lines of water vapor have been previously performed [2]. The first absorption line for water occurs at a frequency of about 600 GHz. Below this frequency water vapor is transparent to the incident radiation. Our spectra occur in the frequency range of 0-250 GHz, and the observed dropout region was about 75-125 GHz. Clearly, water vapor is not the culprit. If this technique were to be applied to much shorter bunch lengths, around 300 fs, then the effects of water vapor should be taken into account. We are unable to rule out other contaminants that may have been present in the air interfering with the measurement process.

The second problem that was investigated was the pyroelectric detectors themselves. The spectral resolutions of the detectors are influenced by a variety of factors. The surface of the detectors is coated by a black film. InfraTec, the manufacturer of our detectors, explain that this coating converts the incoming radiation into heat [3]. One of the pyroelectric detectors in use had its coating accidentally removed at some point prior to our experiments. We do not know for sure how this affected the resolution of the pyroelectric detector, but there does remain some suspicion that this could cause problems. An older style detector that we have on hand does have a similar black coating, but the coating seems to only help response in the 10-30 THz region [4]. It is believed that the same holds for our detectors. Later scans seemed to have no problem with frequencies in the range of 75-125 GHz, which seems to rule out detector coating differences as a source of our problems. We are interested in using an older style of detector to see if the similar issues occur. The drawback is that the InfraTec pyroelectric detectors were designed to eliminate self-interference that was present in the older style of detector. Other parameters that effect the measurement, but that we do not understand, are the size of the detecting elements and the shape of the horns that collect the incoming radiation and deliver it to the detecting element. Further studies of these parameters need to be performed.

A new automated beam control program was recently created for the A0 Photoinjector and is in testing. The goal of the program is to deliver bunches down the center of the beam path at every beam position monitor point. This program will eliminate some of the variations that were beyond our ability to control and compensate for. Hopefully, this will allow for more reproducible results in the future. Future research that needs to be performed includes having the pyroelectric detectors spectral response measured, trying other types of detectors such as Schottky diodes, modeling collector

horn and detector element size effects, and trying to simulate wakefield effects on the measurement process.

References

[1] Lars Fröhlich (Hamburg U.). DESY-THESIS-2005-011, Jun 2005. 56pp. Ph.D. Thesis

<http://tesla.desy.de/~lfroehli/download/Fro05.pdf>

[2] Kabetani, Y.; Nakamura, R.; Yokoyama, S.; Yasui, T.; Araki, T., "Terahertz Time-domain Spectroscopy of Water Vapor Based on Asynchronous Optical Sampling," *Lasers and Electro-Optics - Pacific Rim, 2007. CLEO/Pacific Rim 2007. Conference on*, vol., no., pp.1-2, 26-31 Aug. 2007

<http://ieeexplore.ieee.org/iel5/4391083/4391084/04391789.pdf?tp=&isnumber=&arnumber=4391789>

[3] InfraTec. Pyroelectric Detector.

<http://www.infratec.co.uk/thermography/pyroelectric-detector.html>

[4] Molelectron Detector, Inc. P4-30/P4-40 Low Noise Instruments.

<http://www.coherent.com/downloads/P430P440DataSheet.pdf>

[5] [Marc Alexander Geitz](#) (Hamburg U.) . DESY-THESIS-1999-033, Nov 1999. 182pp. Ph.D. Thesis (Advisor: P. Schmuser).

http://www-library.desy.de/preparch/desy/scan/in_progress/desy-thesis-1999-033.pdf